

Air quality across a European hotspot

Masiol, Mauro; Squizzato, Stefania; Formenton, Gianni; Harrison, Roy; Agostinelli, A.

DOI:

[10.1016/j.scitotenv.2016.10.042](https://doi.org/10.1016/j.scitotenv.2016.10.042)

License:

Creative Commons: Attribution-NonCommercial-NoDerivs (CC BY-NC-ND)

Document Version

Peer reviewed version

Citation for published version (Harvard):

Masiol, M, Squizzato, S, Formenton, G, Harrison, R & Agostinelli, A 2017, 'Air quality across a European hotspot: spatial gradients, seasonality, diurnal cycles and trends in the Veneto region, NE Italy', *Science of the Total Environment*, vol. 576, pp. 210-224. <https://doi.org/10.1016/j.scitotenv.2016.10.042>

[Link to publication on Research at Birmingham portal](#)

General rights

Unless a licence is specified above, all rights (including copyright and moral rights) in this document are retained by the authors and/or the copyright holders. The express permission of the copyright holder must be obtained for any use of this material other than for purposes permitted by law.

- Users may freely distribute the URL that is used to identify this publication.
- Users may download and/or print one copy of the publication from the University of Birmingham research portal for the purpose of private study or non-commercial research.
- User may use extracts from the document in line with the concept of 'fair dealing' under the Copyright, Designs and Patents Act 1988 (?)
- Users may not further distribute the material nor use it for the purposes of commercial gain.

Where a licence is displayed above, please note the terms and conditions of the licence govern your use of this document.

When citing, please reference the published version.

Take down policy

While the University of Birmingham exercises care and attention in making items available there are rare occasions when an item has been uploaded in error or has been deemed to be commercially or otherwise sensitive.

If you believe that this is the case for this document, please contact UBIRA@lists.bham.ac.uk providing details and we will remove access to the work immediately and investigate.

1
2
3
4
5
6 **AIR QUALITY ACROSS A EUROPEAN**
7 **HOTSPOT: SPATIAL GRADIENTS,**
8 **SEASONALITY, DIURNAL CYCLES AND**
9 **TRENDS IN THE VENETO REGION, NE ITALY**
10

11 **Mauro Masiol^{a,b,*}, Stefania Squizzato^{a,c}, Gianni**
12 **Formenton^d, Roy M. Harrison^{b,§}, Claudio Agostinelli^e**
13

14
15 ^a **Center for Air Resources Engineering and Science, Clarkson University, Box**
16 **5708, Potsdam, NY 13699-5708, United States**

17 ^b **Division of Environmental Health and Risk Management, School of**
18 **Geography, Earth and Environmental Sciences, University of Birmingham,**
19 **Edgbaston, Birmingham B15 2TT, United Kingdom**

20 ^c **Dipartimento Scienze Ambientali, Informatica e Statistica, Università Ca’**
21 **Foscari Venezia, Campus Scientifico via Torino 155, 30170 Venezia, Italy**

22 ^d **Dipartimento Regionale Laboratori, Agenzia Regionale per la Prevenzione e**
23 **Protezione Ambientale del Veneto, Via Lissa 6, 30174 Mestre, Italy**

24 ^e **Dipartimento di Matematica, Università degli Studi di Trento, via**
25 **Sommarive 14, Povo, Trento, Italy**

* To whom correspondence should be addressed.
Email: mauro.masiol@gmail.com

§ Also at: Department of Environmental Sciences / Center of Excellence in Environmental Studies, King Abdulaziz University, PO Box 80203, Jeddah, 21589, Saudi Arabia.

27 **ABSTRACT**

28 The Veneto region (NE Italy) lies in the eastern part of the Po Valley, a European hotspot for air
29 pollution. Data for key air pollutants (CO, NO, NO₂, O₃, SO₂, PM₁₀ and PM_{2.5}) measured over 7
30 years (2008/2014) across 43 sites in Veneto were processed to characterise their spatial and
31 temporal patterns and assess the air quality. Nitrogen oxides, PM and ozone are critical pollutants
32 frequently breaching the EC limit and target values. Intersite analysis demonstrates a widespread
33 pollution across the region and shows that primary pollutants (nitrogen oxides, CO, PM) are
34 significantly higher in cities and over the flat lands due to higher anthropogenic pressures. The
35 spatial variation of air pollutants at rural sites was then mapped to depict the gradient of background
36 pollution: nitrogen oxides are higher in the plain area due to the presence of strong diffuse
37 anthropogenic sources, while ozone increases toward the mountains probably due to the higher
38 levels of biogenic ozone-precursors and low NO emissions which are not sufficient to titrate out the
39 photochemical O₃. Data-depth classification analysis revealed a poor categorization among urban,
40 traffic and industrial sites: weather and urban planning factors may cause a general homogeneity of
41 air pollution within cities driving this poor classification. Seasonal and diurnal cycles were
42 investigated: the effect of primary sources in populated areas is evident throughout the region and
43 drives similar patterns for most pollutants: road traffic appears the predominant potential source
44 shaping the daily cycles. Trend analysis of experimental data reveals a general decrease of air
45 pollution across the region, which agrees well with changes assessed by emission inventories. This
46 study provides key information on air quality across NE Italy and highlights future research needs
47 and possible developments of the regional monitoring network.

48

49 **Keywords:** air pollution, nitrogen oxides, particulate matter, Veneto, trends.

50

51

52

53 1. INTRODUCTION

54 Since the mid-90s, the European Community has adopted increasingly stringent standards for
55 abating emissions and for improving the air quality. The main steps in the legislative process were
56 the Framework Directive 96/62/EC, its subsequent daughter Directives and the more recent
57 Directive 2008/50/EC. As a consequence, a general improvement of air quality has been recorded in
58 the last decade. However, current and future EU standards are still breached in some European
59 regions, the so-called hotspots, e.g., Northern Italy, Benelux and some Eastern Countries (Putaud et
60 al., 2004;2010). Under this scenario, the development of additional successful strategies for
61 emission mitigation and the implementation of measures for air quality control are two major
62 questions addressed by policy makers and in scientific research, respectively.

63

64 Following the implementation of the EC Directives, local and national authorities are required to
65 monitor air quality. Measurement data are primarily managed by local agencies to assess the extent
66 of air pollution, check if standards are complied with, and, in case of the exceeding of Limit Values
67 or even lower assessment thresholds, to inform the population about potential health impacts.
68 Beyond their original regulatory purpose, such data also represent a valuable resource: if historical
69 data are available, long-term trends can be investigated to obtain real feedback upon the successes
70 and failures of past and current mitigation strategies.

71

72 The Po Valley (N Italy) is neither a city nor an administrative unit, but it can be considered a
73 megacity (Zhu et al., 2012). Currently, it is one of the few remaining and most worrying European
74 hotspots: high levels of hazardous pollutants are commonly recorded over a wide area ($\sim 48 \cdot 10^3$
75 km^2) hosting ~ 16 million inhabitants. The anthropogenic pressure and some peculiar
76 geomorphological features (a wide floodplain is enclosed by the Alps and Apennine mountains)
77 lead to frequently breaches of limit and target values imposed by EU Directives (EEA, 2016) for
78 nitrogen oxides, ozone and particulate matter (PM).

79 The Veneto Region (Figure 1) is located in the eastern part of the Po Valley and extends over
80 $\sim 18.4 \cdot 10^3 \text{ km}^2$ ranging from high mountain environments (29% of the territory), to intermediate hill
81 zones (15%), large and flat plain areas (56%) and $\sim 95 \text{ km}$ -long coastlines. From an administrative
82 point of view, it is subdivided in 7 Provinces: Belluno (BL), Treviso (TV), Vicenza (VI), Venice
83 (VE), Padova (PD) and Rovigo (RO). Heavy anthropogenic pressures are present almost
84 continuously: a total of $\sim 4.9 \cdot 10^6$ inhabitants are resident in some large cities ($> 2 \cdot 10^5$ inhabitants:
85 Verona, Padova and Venice-Mestre) and in a number of minor towns and villages which form a
86 continuum “sprinkled” network of urban settlements. Consequently, emissions from road traffic and
87 domestic heating are spread throughout the region. Some industrial areas are also present, mainly
88 close to the main cities and with distinctive features and different plant types. In addition, the
89 Veneto lies in a strategic location linking Central, Eastern Europe and continental Italy: a dense
90 network of international E-roads and transport hubs attract large amounts of road and intermodal
91 traffic, mostly heavy duty diesel-powered trucks. A large percentage of the region includes
92 agricultural fields, mostly located in the plain (intensive farming) and hilly areas (vineyards,
93 orchards), while rural environments are present mainly in hilly and mountain regions. A land use
94 map is provided in Figure 1: this composite landscape inevitably makes the emission scenario of the
95 region extremely complex and its spatial variations quite unpredictable.

96
97 This study aims to examine and describe the spatial variations, temporal trends and seasonality of
98 air quality across the Veneto Region over 7 years (2008-2014). Datasets used in this study include
99 the mass concentration of key air pollutants as required by European air quality standards: nitrogen
100 oxides ($\text{NO} + \text{NO}_2 = \text{NO}_x$), ozone (O_3), carbon monoxide (CO), sulphur dioxide (SO_2) and PM with
101 aerodynamic diameter less than $10 \text{ }\mu\text{m}$ (PM_{10}) and less than $2.5 \text{ }\mu\text{m}$ ($\text{PM}_{2.5}$). Air quality data were
102 measured by ARPAV (Veneto Environmental Protection Agency) through a well-established
103 network of 43 sampling stations (ARPAV, 2014) covering a large portion of the territory (Figure 1).
104 A series of chemometric procedures are used to assess the extent of air pollution, to verify the

effectiveness of site categorization and to find patterns commonly recorded across the Veneto or identify sites with anomalous pollution levels. The gradients of concentrations are depicted and seasonal/diurnal/weekly patterns are investigated. The long-term trends are seasonally decomposed and then processed to find the general orientations and drifts in air pollution over sites with a different categorization. Furthermore, long-term trends are coupled with changes in the emission inventories to verify if estimated emissions match with experimentally recorded levels of key air pollutants across the region.

112

113 **2. MATERIALS AND METHODS**

114 **2.1 *Sampling sites***

The map of sites is shown in Figure 1, while Table 1 summarises their general characteristics and measured pollutants. Figure 1 also shows the political, relief and land use maps. Sites are identified by the initials for the province and their category. Sites were selected to fulfil some specifications: (i) data availability must cover at least four years in 2008/14; (ii) sites must be representative of most important pollution climate scenarios, such as citywide pollution, regional background or traffic and industrial hotspots and (iii) sites must be representative of differing environments (mountain, hilly, plain, coastal areas). In particular:

- 122 • At least one site was selected as rural background (RUR sites) for each Province (total 9 sites),
123 i.e. in areas not directly influenced by trafficked roads and/or urban and industrial settlements. In
124 particular, BL.RUR and VI.RUR are located in remote locations at high altitudes. RUR sites are
125 fundamental to assess the background gradients at the regional scale;
- 126 • Eighteen sites were categorised as suburban (SUB) and urban (URB), i.e. broadly representative
127 of citywide levels of air pollutants;
- 128 • A total of 8 sites were selected as representative of traffic hotspots (TRA) and placed at kerbside
129 locations in cities experiencing heavy traffic and/or frequent road congestion events;

130 • Eight sites were set as representative of main industrial (IND) areas. Each site has peculiar
131 characteristics. VE.IND is located downwind of Porto Marghera, one of the main industrial
132 zones in Italy extending over $\sim 12 \text{ km}^2$ and including a large number of different installations
133 (thermoelectric power plants burning coal, gas and refuse derived fuels, a large shipbuilding
134 industry, an oil-refinery, municipal solid waste incinerators and many other chemical,
135 metallurgical and glass plants). VI.IND1 and VI.IND2 are representative of small and medium-
136 sized tannery industries, PD.IND1 and PD.IND2 are set in an area potentially affected by a
137 municipal solid waste incinerator plant, PD.IND3 was selected to monitor the fall-out from a
138 steel mill and VR.IND and PD.IND4 are representative of emissions from cement plants.

139

140 2.2 *Experimental*

141 All selected sites are equipped with fully automatic analysers set to collect data on hourly (gaseous
142 pollutants) or hourly/bihourly bases (PM_{10} and $\text{PM}_{2.5}$). QA/QC of measurements is guaranteed by
143 ARPAV internal protocols, which fully comply with the standards required by EC Directives in-
144 force: EN 14626:2012 for CO, EN 14211:2012 for NO, NO_2 , and NO_x , EN 14212:2012 for SO_2 ,
145 EN 14625:2012 for O_3 . CO, NO_x , O_3 and SO_2 instruments were calibrated every day. Hourly- or
146 bihourly- resolved PM_{10} and $\text{PM}_{2.5}$ were measured with beta gauge monitors: validation
147 experiments were routinely conducted between gravimetric (EN 14907:2005) and automatic
148 methods; several tests were also performed routinely (at least 1 test every week) to keep a constant
149 check on the beta gauge samplers. Pairs of filters were measured with both methods and the results
150 were checked to ensure that they are within the variation margins imposed by the technical
151 protocols adopted in UNI EN 12341:2001. Some sites were not equipped with hourly PM monitors
152 (Table 1), but may provide daily gravimetric-measured PM_{10} levels. In this case, PM was collected
153 by low-volume samplers on filters and the mass concentration was measured by gravimetric
154 determination (EN 14907:2005) at constant temperature ($20 \pm 5^\circ\text{C}$) and relative humidity (RH,

155 50±5%). Consequently, no diurnal patterns are investigated in such sites, but only interannual and
156 seasonal trends.

157

158 **2.3 *QA/QC and data handling***

159 Data have been validated by ARPAV through a well consolidated internal protocol (ARPAV, 2014)
160 and according to the European standards. The full dataset was therefore used for exploratory
161 statistics. However, the aim of this study is to detect the general behaviour of air pollution and some
162 clearly identified high pollution episodes which occurred in 2008/14 across the region. Examples
163 are the burning of a thousand folk fires on the eve of Epiphany (Masiol et al., 2014a) or fireworks
164 for Christmas and other local celebrations. Consequently, preliminary data handling and clean-up
165 are carried out to check the datasets for robustness, outliers and anomalous records. For this
166 purpose, data greater than the 99th percentile were included for exploratory analysis but not in the
167 trend estimation. Data were also adjusted to account for the shift in anthropogenic emissions due to
168 the changes between local time (UTC+1) and daylight savings time (DST). This latter correction
169 helps in investigating daily patterns of anthropogenic emission sources.

170

171 Data were analysed using R (R Core Team, 2016) and a series of supplementary packages,
172 including ‘openair’ (Carslaw and Ropkins, 2012; Carslaw, 2015), ‘PMCMR’ (Pohlert, 2015) and
173 ‘localdepth’ (Agostinelli and Romanazzi, 2011;2013).

174

175 **2.4 *Data depth classification analysis***

176 A classification analysis was used to check the accuracy of the site categorisation, i.e., to verify
177 whether the sampling sites in a category (RUR, SUB+URB, TRA, IND) are characterised by a
178 general homogeneity in air pollutant levels. This task is accomplished by applying a new
179 classification technique based on statistical data depth (DD). This technique is well reviewed
180 elsewhere (Mosler and Polyakova, 2012 and the reference therein) and recently was extended to

functional and multivariate data (Ramsay and Silverman, 2006; Lopez-Pintado and Romo, 2009; Lopez-Pintado and Romo, 2011; Claeskens et al., 2014; Cuevas, 2014).

The depth of a point relative to a given dataset measures how deep the point lies in the data cloud, i.e. it measures the centrality of a point with respect to an empirical distribution (Mosler and Polyakova, 2012). DD provides an order to the observations and the rank system provided by DD can be used to perform unsupervised and supervised classification analysis. A statistical depth function should be invariant to all (non-singular) affine transformations; it reaches the maximum value at the centre of symmetry for symmetric distribution and it becomes negligible when the norm of the point tends to infinity. Another important property is ray-monotonicity, i.e. the statistical depth does not increase along any ray from the centre (Liu, 1990; Zuo and Serfling, 2000). The classical notion of data depth has been extended to functional data and the different available implementations aim to describe the degree of centrality of curves with respect to an underlying probability distribution or a sample. Some advisable properties of functional depths are the (semi-) continuity, the consistency, and the invariance under some class of transformations, which tends to vanish when the norm of a curve tends to infinity (Mosler and Polyakova, 2012).

A classification analysis was performed by using the DD-plot tool and a functional multivariate simplicial depth. First, a (empirical) simplicial depth of a *point* y with respect to a *set of points* $x = (x_1, \dots, x_n)$ in the Euclidean space of dimension p is introduced. $S_i = S(x_{i1}, x_{i2}, \dots, x_{ip}, x_{ip+1})$ represents the simplex obtained using $p+1$ points in the sample. A simplex of $p+1$ points in a space of dimension p is the convex hull of those points. Then $d(y; x_n)$ is the fraction of simplicials S_n contains y overall combinations of the $p+1$ indices $i_1, i_2, \dots, i_p, i_{p+1}$ in the set $1, \dots, n$. This is a consistent estimator of the simplicial depth, which is the probability that a random simplex $S(X_1, X_2, \dots, X_p, X_{p+1})$ will cover the *point* y when $X_1, X_2, \dots, X_p, X_{p+1}$ are identical and independent copies of the random variable X from where the sample is drawn.

207 Thus, we can consider a set of (multivariate) curves $x_j(t)$, ($j=1, \dots, J$) measured at time t_1, t_2, \dots, t_N ,
 208 i.e. $x_j(t_j)$ is a point in the Euclidean space of dimension p . In our context, $x_j(t)$ is the multivariate
 209 time series at location j (sampling site) for a set of p pollutants concentration measured at time t .
 210 Following Claeskens et al. (2014), we defined the depth of a given curve $y(t)$ according to the
 211 sample $x=(x_1(t), \dots, x_J(t))$, denoted $d(y(t), x)$ as the weighted average of the empirical simplicial
 212 depth evaluated at any given time t_1, t_2, \dots, t_N . The weights proportional to the fraction of available
 213 observations at each time is then set. This is important to be considered for the presence of missing
 214 values.
 215
 216 The classification is performed using the depth-versus-depth plot (DD-plot) (Li et al., 2012; Cuevas,
 217 2014). Considering two groups of curves $x=(x_1(t), \dots, x_J(t))$ and $z=(z_1(t), \dots, z_K(t))$, the goal is to
 218 classify a curve $y(t)$ in one of these. Hence, we evaluate $d(y(t),x)$ and $d(y(t),z)$ that represents the
 219 depth of $y(t)$ according to x and to z . We assign $y(t)$ to the first group if $d(y(t),x) > d(y(t),z)$ and to
 220 the second group otherwise. In particular, two groups of curves will be well separated if $d(x_j(t),x) >$
 221 $d(x_j(t),z)$ for each observation x_j and $d(z_k(t),x) < d(z_k(t),z)$ for each observation z_k . Finally, we can
 222 plot on a Cartesian axis the points $(d(x_j(t),x), d(x_j(t),z))$, $j=1, \dots, J$ and the points $(d(z_k(t),x), d(z_k(t),z))$,
 223 $k=1, \dots, K$, i.e. the DD-plot. Curves (sampling sites) well classified in the first group will be plotted
 224 at the right bottom corner of the graphics, whereas curves well classified in the second group will
 225 appear at the left upper corner. Curves equally well classified in both groups will lie around the
 226 bisector line of the plot.
 227
 228 In this study, four site categories are used to group the sites: rural (RUR), urban and sub-urban
 229 (URB), traffic (TRA) and industrial (IND). For each couple of categories, the DD-plots are
 230 evaluated on the basis of distributions of one or more pollutants.
 231
 232

233 3. RESULTS

234 A summary of data distributions during the whole study period (all available data) is provided as
235 boxplots in Figure 2 and maps in Figures SI1. Concentrations are expressed as mass concentration;
236 NO_x is expressed as NO₂, as required by EU standards. Moreover, Table SI2 reports annual average
237 concentration and exceedances for NO₂, O₃, PM₁₀ and PM_{2.5}. CO and SO₂ are not included because
238 no exceedances were observed.

239

240 3.1 *Carbon monoxide and sulphur dioxide*

241 In Veneto, CO and SO₂ are not critical pollutants. CO values are well below the EC limit value and
242 WHO guidelines (WHO, 2000), i.e. 10 mg m⁻³ as daily maximum over eight hours. The highest
243 hourly average levels of CO over six years were recorded at VR.URB1, PD.IND2, VR.TRA3,
244 PD.URB, VE.TRA1 and PD.IND1 (all ~0.6 mg m⁻³); remaining sites showed concentrations
245 between 0.2 and 0.6 mg m⁻³.

246

247 SO₂ does not show exceedances of European standards both for hourly averages (350 µg m⁻³) and
248 for 24-h averages (125 µg m⁻³). The 2008/14 average concentrations across Veneto were very low,
249 ranging from ~0.6 µg m⁻³ (often below instrumental detection limits) at VI.URB3 and RO.SUB to
250 ~4 µg m⁻³ at some sites near Venice (VE.IND, VE.URB1). The higher levels in Venice sites can be
251 likely associated to harbour and industrial emissions (i.e. thermal power plant, oil refinery and
252 municipal solid waste incinerator). While the contribution of the harbour to the levels of SO₂ in
253 Venice is still debated (Contini et al., 2015), the role of industrial emissions is well supported by the
254 emission inventories. In 2005, about 76% of overall SO₂ emissions in the Veneto were released in
255 the Province of Venice, of which 69% (19,742 Mg y⁻¹) came from combustion in energy and
256 transformation industries (ARPAV, 2011).

257

258

259 3.2 *Nitrogen oxides*

260 When considering the short-term metrics, NO₂ does not represent a special risk for human health in
261 Veneto: the 1-hour alert threshold of 400 µg m⁻³ was never breached, while the 1-hour average of
262 200 µg m⁻³ not to be exceeded more than 18 times over a calendar year was exceeded only at
263 VR.TRA3 in 2008. However, NO_x becomes pollutants of concern when looking at the long-term
264 metrics. The minimum average levels were found at two rural sites located in high mountain
265 environments, while maxima were measured at a traffic site in Verona located very close to a
266 logistic intermodal freight transport hub spanning over 4 km² and moving 26 million tons of goods
267 annually (VR.TRA3). The average concentrations of NO varied from 0.5-0.6 µg m⁻³ (VI.RUR,
268 BL.RUR1) to 50 µg m⁻³ (VR.TRA3), while NO₂ ranged from 4 µg m⁻³ (BL.RUR1) to 53 µg m⁻³
269 (VR.TRA3) and NO_x from 5 µg m⁻³ (BL.RUR1) to 130 µg m⁻³ (VR.TRA3). Comparing results
270 averaged over 2008/14 with the annual EC limit value for NO₂ (40 µg m⁻³ averaged over one year),
271 the limit was substantially exceeded at six traffic sites (VE.TRA2, VE.TRA1, VI.TRA, VR.TRA2,
272 PD.TRA, VR.TRA3).

273

274 3.3 *Ozone*

275 In rural sites, average O₃ levels ranged from 48 µg m⁻³ (RO.RUR) to more than 90 µg m⁻³
276 (BL.RUR1, VI.RUR), while urban and suburban sites varied between ~40 and ~60 µg m⁻³. Despite
277 the low number of sites measuring ozone in traffic and industrial environments, it is evident that
278 polluted environments generally exhibit the lower average concentrations: the minimum levels were
279 recorded at VR.TRA3 (36 µg m⁻³), which, inversely, shows the higher NO concentrations (it leads
280 close to a large logistic intermodal freight transport hub and, thus, it is affected by heavy traffic of
281 diesel-powered trucks).

282

283 Ozone is the subject of several regulations: the alert threshold (maximum 1-hour level of 240 µg
284 m⁻³) was never breached in 2008-2012, but was exceeded five times in 2013 at PD.RUR1. This

285 result recalls the anomaly of PD.RUR1 already reported for PM₁₀-bound polycyclic aromatic
286 hydrocarbons (Masiol et al., 2013). Despite PD.RUR1 being originally located far from direct
287 emission sources, it probably suffers from a local unknown source of air pollution. In addition, it is
288 located between and equidistant from three main urban settlements (Mestre, Padova and Treviso).
289 Further studies should be carried out to detect the potential sources; in the meanwhile, its
290 categorisation should be revised.

291

292 The information threshold ($180 \mu\text{g m}^{-3}$ over one hour) was frequently exceeded at most of the sites.
293 VI.RUR deserves special attention because it is affected annually by 39–126 exceedances; it is
294 located in a remote area (1366 m a.s.l.) characterised by grass- and wood-lands and is not affected
295 by direct anthropogenic sources. Consequently, high O₃ levels may be linked to the transport of air
296 masses containing ozone or ozone-precursors from the nearby highly populated plain areas or to the
297 local biogenic emission of ozone-precursors from plants. In addition, since this area is not impacted
298 by traffic, titration of photochemically produced ozone by primary NO is negligible.

299

300 The EC long-term target value of $120 \mu\text{g m}^{-3}$ and the WHO air quality guideline of $100 \mu\text{g m}^{-3}$
301 measured as maximum daily 8 hour running averages (not to be exceeded more than 25 days over 3
302 years for the EC target) were also frequently breached at almost all the sites. Similarly, the long
303 term objective value for the protection of vegetation (AOT40) calculated over the warm period
304 (May to July) is also amply breached at all the rural sites, posing a serious risk to high-quality
305 agriculture promoted by regional policies.

306

307 It is therefore evident that ozone is a critical pollutant across the Veneto. The standards for ozone
308 are more difficult to achieve across the warmer regions (southern Europe) because of the larger
309 magnitude of summer photochemical O₃ episodes. In addition, O₃ levels are also influenced
310 substantially by the extent of reactions with local NO emissions, which are currently falling in

311 Europe (Colette et al., 2011) in order to comply with the increasingly stringent emission standards
312 required for road vehicles. As a result, recent decreases in NO emissions across Europe may limit
313 reaction with O₃, which is the main sink of O₃ in the polluted atmosphere.

314

315 **3.4 *NO_x partitioning and total oxidants (OX)***

316 Recent changes in emission trends for some air pollutants and the complex photochemistry of the
317 NO-NO₂-O₃ system are further evaluated through two derived parameters. The partitioning of
318 nitrogen oxides was investigated through the NO₂/NO_x ratio (Figure 2 and Figure SI1b) and total
319 oxidants (OX=NO₂+O₃, expressed as ppb) are often used to describe the oxidative potential (Kley et
320 al., 1999; Clapp and Jenkin, 2001). Results are highly variable, but higher ratios are generally
321 recorded at rural sites because of the lower primary NO emissions. The average levels of OX show
322 little variation across the Region with distributions typically showing interquartile ranges between
323 25 and 50 ppbv. The highest site averages are seen at rural sites due to photochemical ozone
324 creation, and at traffic sites, presumably caused by high emissions of primary NO₂.

325

326 **3.5 *Particulate matter***

327 PM₁₀ and PM_{2.5} are critical air pollutants in Veneto. Average PM₁₀ levels over 2008/14 varied from
328 less than 20 µg m⁻³ in BL.RUR2 and VR.RUR to more than 40 µg m⁻³ in VI.URB1 and VI.TRA.
329 Some sites breached the European annual limit value of 40 µg m⁻³ (PD.IND3, VI.URB1, PD.URB,
330 VR.TRA2, VE.TRA1, PD.TRA and PD.IND1), except in 2013 and 2014 when no exceedances
331 were recorded. In such sites, the annual average concentrations are usually close to the European
332 limit value: this way, small fluctuations in PM10 levels may have a large effect in marking them as
333 “fulfilling” or “not fulfilling” the EC standard. However, every year more than 20 sites exceeded
334 the daily mean of 50 µg m⁻³ for more than 35 times in a calendar year. Among these sites,
335 VI.URB1, VE.TRA2, VE.IND and VE.URB3 showed the highest number of daily exceedances for
336 a minimum of 77, 66, 64 and 60 times in a calendar year, respectively.

337

338 The PM_{2.5} monitoring network started its operation in 2009, when the Directive 2008/50/EC entered
339 into force, and continued to grow over the following years. This way, only 8 sites provide sufficient
340 data to be included in this study. The annual limit value (25 µg m⁻³) was frequently breached (five
341 years out of six) at PD.URB, PD.IND1, PD.IND2, VE.IND and VI.URB1. Similar to PM₁₀, in 2013
342 only 6 stations breached the annual average value, while no exceedances were recorded in 2014.

343

344 4. DISCUSSION

345 4.1 *Differences among sites*

346 Maps showing the average levels of recorded pollutants over the 2008/14 period are reported in
347 Figures SIIa,b for different site categories. Levels of CO are generally low across the region and do
348 not show any evident trend among site categories. On the contrary, nitrogen oxides, SO₂, PM₁₀ and
349 PM_{2.5} show levels increasing from rural to urban to traffic sites, while concentrations in industrial
350 sites are highly variable and reflect the specific characteristics of each site (Figure 2). Such patterns
351 are opposite to ozone (higher levels at rural sites in high mountain environments and lower at sites
352 polluted with primary emissions).

353

354 Motor vehicles are major sources of NO (Keuken et al., 2012; Kurtenback et al., 2012) and a series
355 of volatile organic compounds (VOCs) (Gentner et al., 2013). Munir et al. (2012) have shown that
356 emissions from cars, buses and heavy vehicles have strong effects on urban decrements of ozone
357 levels. Due to this, the lower O₃ levels in most anthropogenically affected sites in Veneto are related
358 to the primary emissions of NO. This fact is further well supported by the partitioning of nitrogen
359 oxides (Figure SIIb): lower NO₂/NO_x ratios are recorded at urban and hot-spot sites, indicating that
360 high relative concentrations of NO lead to ozone depletion. Another reason is linked to the impact
361 of natural sources of VOCs, such as biogenic isoprene and terpenes, i.e. known effective ozone-
362 precursors (Duane et al., 2002). The land cover map (Figure 1) shows that the hilly and mountain

363 areas of N Veneto are covered by forests. Thus, biogenic VOCs are expected to be elevated in rural
364 and mountain environments and enhance the generation of ozone. In this context, modelling studies
365 in Europe indicate that biogenically-driven O₃ accounts for ~5% in the Mediterranean region (Curci
366 et al., 2009).

367

368 The Kruskal-Wallis analysis of variance by ranks (KW_{test}) was applied as a global non-parametric
369 test for depicting statistically significant inter-site variations. The null hypothesis is rejected for
370 $p < 0.05$, meaning that the sites in a category are statistically different. In this case, the post-hoc test
371 after Nemenyi (Demšar, 2006) was applied for multiple sample comparison to point out the pairs of
372 sites which differ significantly in the pollutant level. Generally, results indicated that air pollutants
373 are uniformly distributed across the region: no pairs of sites differ in the levels of CO, while only
374 the two remote RUR sites (BL.RUR1 and VI.RUR) present statistically significant differences for
375 NO_x and ozone from a large number of other sites. The application of comparison tests for PM₁₀ is
376 complicated by the lack of data at the two remote sites and by the availability of differently time
377 resolved data (hourly and daily). Despite such limitations, results indicate that only BL.RUR2
378 exhibits significantly lower concentrations than other sites.

379

380 **4.2 Differences amongst site categories**

381 KW tests indicated that the concentrations of many pollutants measured across the Veneto are
382 statistically similar even at sites which are categorised differently (except for the two sites located
383 in extremely remote mountain areas). Moreover, the results point to an important conclusion: air
384 pollutants are almost uniformly distributed across the region. However, these results also indicate
385 that there is an apparent homogeneity amongst sites, i.e. sites having different categorisation may
386 experience statistically similar levels of air pollutants. This hypothesis was tested statistically using
387 data depth (DD) analysis. However, there are some limitations to its application: the important
388 fraction of missing data for some pollutants/sites and the lack of the full set of pollutants at most

389 sites limits the possibilities for its use. Therefore, data-depth classifications were separately
390 performed for: NO, NO₂ and NO_x, (ii) PM₁₀, (iii) CO. Since few TRA and IND sites measured O₃
391 and SO₂, the DD analysis was not possible for these pollutants because not all the site categories
392 would be adequately represented. Application to one or a few pollutants has the disadvantage of
393 processing pollutants separately; however, it also has the advantage that it ensures the presence of a
394 reasonable high number of sites, which make the results more robust and the spatial extent of the
395 analysis more extensive.

396

397 The DD classification for nitrogen oxides (Figure 3) shows that most of RUR and URB sites are
398 generally well separated, i.e. they are plotted far from the 1:1 bisecting line. Rural sites are also well
399 separated from traffic and industrial ones. However, some exceptions are found. BL.SUB,
400 VI.URB3, VI.URB4 and RO.SUB are more similar to RUR than to URB sites, i.e. NO_x levels are
401 generally lower than other urban sites, as also confirmed by boxplots in Figure 2. On the contrary,
402 PD.RUR1 and RO.RUR lie on the URB-side of the DD plot, i.e. they are more comparable to URB
403 than RUR sites. Although the anomalously high levels of air pollution at PD.RUR1 were already
404 recognised and discussed (Masiol et al., 2013), this result also shows that two rural sites probably
405 experience relatively high levels of NO_x with respect to remaining RUR sites.

406

407 Although levels of pollutants in sites categorized as rural generally differ from other categories,
408 there is not a clear separation among URB, TRA and IND sites. In fact, the DD classification
409 analysis has demonstrated that most of the TRA and IND sites can be grouped with URB sites
410 (points lay around the bisector of the plot). DD-plots of PM₁₀ also show this behaviour, while no
411 clear classification was possible using CO (Figure SI2 and SI3), i.e. CO levels are quite similar at
412 all site categories.

413

414 EU directives assume that URB sites are representative of the exposure of the general population,
415 while TRA and IND sites should be representative of areas where the highest concentrations may
416 occur. However, results show that this condition is rarely fulfilled in Veneto. In this context, a
417 recent position paper (JRC-AQUILA, 2013) has pointed out the need to implement criteria for
418 improving the classification and representativeness of air quality monitoring stations in Europe.
419 There are several reasons that may explain failure of the classification:

- 420 • The widespread distribution of emissions. Since the flat areas of the Po Valley host a ‘sprinkled’
421 continuum of urban settlements with different sizes, densities and uses (Romano and Zullo,
422 2015), the rather constant presence of anthropogenic emissions leads to a widespread distribution
423 of emission sources. As a consequence, air pollutants emitted by different sources mix in the
424 atmosphere and the limited atmospheric circulation in Po Valley further limits their dispersion.
- 425 • The similarity of URB and TRA sites probably results from urban planning. Most large cities
426 have ancient origins and contain medieval or even Roman city centres with historic buildings
427 and narrow streets. A rapid and intense urbanization was experienced in Italy after World War II
428 with fast build-up of large urban/suburban areas all around the ancient city centres, often without
429 a well-informed approach to urban planning. Consequently, some city configurations
430 inevitably limit the movement of road traffic and are characterised by busy streets which are
431 frequently congested during rush hour periods, i.e. when traffic is widespread over the city
432 centres and not properly channelled into main orbital or bypass roads. The high density of
433 emissions leads to a high level of pollution from road traffic across cities and to the consequent
434 similar levels of pollutants between URB and TRA sites.
- 435 • The poor differentiation between URB and IND sites may result from the lack of large industrial
436 zones (except in VE). Most of Veneto cities host small and medium-sized industries in several
437 sectors: glass, cement, food products, wood and furniture, leather and footwear, textiles and
438 clothing, gold jewellery, chemistry, metal-mechanics and electronics. Large industrial zones are
439 only present in VE (Porto Marghera). In addition, during the last 20 years, a large number of

companies have relocated their plants abroad, while the global financial crisis (2007/9) has overwhelmed the industrial and economic sectors with a consequent decrease in the production of goods and/or the collapse, closure or downsizing of many companies/industries. Today, small/medium sized industrial areas are scattered across the region, with many of the more significant industries located close to major cities. As a result, some IND sites can be more affected by urban sources than industrial emissions. For example, Porto Marghera, the main industrial area of Veneto, lies SE of the city of Mestre. VE.IND (representative of Porto Marghera) is located just east of the industrial area (Figure SI4). During winter frequent temperature inversions are responsible for the build-up of air pollutants (mostly NO_x, PM) and VE.IND lies just downwind of the urban area of Mestre under prevailing wind regimes (wind rose in Figure SI4), while it is rarely downwind of the industrial area. Consequently, in winter VE.IND is likely to be more affected by the plume from the urban area than by the industrial emissions. This hypothesis is also confirmed by previous studies (Squizzato et al., 2014; Masiol et al., 2012; 2014b), which reported similar concentrations of PM-bound species between VE.IND and the city centre of Mestre. Further modelling studies are needed to inform enhancements to the monitoring network and to better sample the industrial emissions.

4.3 *Spatial gradients*

The characteristics of anthropogenic pressures and the peculiar topography strongly influence the pollutant distribution: this make the quantification of pollutant gradients very challenging. RUR sites can be used as good estimators for determining gradients across the region because they can be considered as representative of the regional pollution as suggested by Lenschow et al. (2001) for PM: they are located away from large sources and are also fairly uniformly distributed across the region. Average concentrations at RUR sites have therefore been spatially interpolated to investigate the gradients of background levels of air pollutants across the region. Semi-variograms were investigated, showing that all pollutants do not all have the same direction, and ordinary

kriging was selected as the best model to interpolate the data. In this study kriging analysis merely aims to shape the background gradients because it was applied over a limited number of points (9). Maps for pollutants recorded at more than six sites (NO_x , O_3 , OX) are provided in Figure 4, while the standard errors of predictions are shown in Figure SI5. All variables show marked gradients. Nitrogen oxides increase from the mountain environments in the north to the coastal plain areas; however the direction of maximum slopes in the increases differ slightly: NO from NW to SE, while NO_2 is from NNW to SSE. The gradient for ozone is opposite to NO , with maximum concentrations at high mountain rural sites and minima in coastal areas. The clear anti-correlation between the gradients of NO and O_3 clearly depicts their relationship: at rural sites, NO emissions from anthropogenic sources are low and therefore, the reaction with ozone is its main sink, and the main sink for ozone. Due to the low concentrations of NO_2 at RUR sites when compared to ozone, gradients for OX are similar to those of ozone.

4.4 *Seasonal patterns*

The monthly-resolved distributions of air pollutants are reported in Figure 5. No evident seasonal patterns are found for the two high-mountain sites (BL.RUR1 ad VI.RUR). At the remaining sites, all the pollutants except SO_2 exhibit clear seasonal cycles. CO , NO , NO_2 , NO_x , PM_{10} and $\text{PM}_{2.5}$ show significantly higher levels in colder months (KW_{test} at $p < 0.05$). Rapid increases occur between mid-September and December; falls in concentration occur between March and mid-April. This pattern can be attributed to the interplay of some covariant causes:

- The lower mixing layer heights in winter, which limit the dispersion of pollutants emitted locally. The typical planetary boundary layer height in the Po Valley is 450 m in winter, and rises up to 1500-2000 m in the warmer months due to the thermal convective activity (Di Giuseppe et al., 2012; Bigi et al., 2012).
- Ambient temperature controls the gas-particulate phase partitioning of semivolatile compounds (ammonium nitrate and part of organic carbon). In Veneto nitrate accounts for $0.1\text{--}0.5 \mu\text{g m}^{-3}$

(0.7–2.5% of PM_{2.5} mass) in August and for 5–10 µg m⁻³ (16–25%) in February (Masiol et al., 2015) and organic carbon in PM_{2.5} varies from about 2.6 µg m⁻³ in June and 11.4 µg m⁻³ in December (Khan et al., 2016).

- Increased emissions in the coldest months mainly driven by increasing energy demand for domestic heating. Domestic heating is regulated at national level: generally, the switching on is fixed to occur on 15 October, while the switching off is on 15 April, i.e. when the fastest changes occur. However, such dates can change according to the weather. Wood smoke from domestic heating may contribute appreciably to higher winter concentrations of PM.
- the drop of actinic fluxes in winter and the consequent reduction of hydroxyl radical, ozone, and the oxidative activity which is a sink for many pollutants.

Ozone shows a strong seasonal pattern. Ozone shows the highest values during the warmest period (generally Apr–Sep), when the solar radiation is higher (Figure 5) and the atmospheric photochemistry is more active. Generally, ozone levels reach approx. 20 µg m⁻³ in winter, but never drop below 50 µg m⁻³ at RUR sites located in high mountain environments (BL.RUR1, VI.RUR, VR.RUR >800 m above sea level). The patterns of OX are dominated by ozone both in rural and polluted sites: the highest levels were reached in the rural mountain sites (BL.RUR1 2020 m asl; VI.RUR 1366 m asl and VR.RUR 824 m asl).

Sulphur dioxide lacks a clear seasonal pattern. Industrial emissions are expected to be quite constant through the year, but highest emissions of SO₂ are may occur in summer due to an increase in energy production from coal power plants to meet air conditioning demand. However, the higher mixing layer height and the enhanced photochemistry driving S(IV) to S(VI) conversion lead to similar concentrations to the cold period.

518

519 **4.5** *Daily and weekly patterns*

520 Figure 6 reports the diurnal cycles, while Figure SI6 shows the weekly patterns. As for the seasonal
521 patterns, daily cycles are the result of interplays among the strength of sources, photochemical
522 processes and weather factors. Although minor changes due to peculiar local conditions are found,
523 almost all the sites exhibit rather similar daily and weekly cycles, except at the three high mountain
524 sites. CO and nitrogen oxides show typical daily cycles linked to road traffic at almost all the sites,
525 with two daily peaks corresponding to the morning and evening rush hours (7–9 am and 6–8 pm).
526 The morning and evening peaks are split by a minimum, which is assumed to be the result of: (i)
527 lower emissions (less traffic); (ii) larger availability of ozone driven by the daylight photolysis of
528 NO_x and the oxidation of VOC and CO (iii) higher convective activity leading to a deeper mixed
529 layer, which enhances the atmospheric mixing. Weekly patterns are also linked to road traffic:
530 generally, average levels increase from Mondays to Thursdays, while a fast drop is measured during
531 weekends, when road traffic reach minimum volumes and heavy duty vehicles over 7.5 tonnes are
532 subject to some limitations (over the whole weekends in summer and on Sundays in winter).

533

534 Ozone and total oxidants (OX) show evident daily peaks in the mid-afternoon, i.e. the hours
535 experiencing the higher solar irradiation, and lower levels are experienced between 6 and 9 am local
536 time (DST time-corrected in summer). These patterns are also enhanced in summer due to the
537 higher solar irradiation. It is evident that daily peaks of OX are delayed 2-3 hours with respect to
538 ozone, corresponding to the increased NO to NO₂ oxidation and primary NO₂ emissions in evening
539 rush hours. The weekly patterns are the mirror images of CO and NO_x with higher concentrations
540 during the weekends, following the drop of fresh anthropogenic emissions. However, such marked
541 diurnal patterns are not found at the three high mountain sites, which show rather constant and high
542 levels throughout the day. This “flatter” pattern has also been observed at other high-mountain sites
543 in the Apennines (Cristofanelli et al., 2007) and Alps (Vecchi and Valli, 1998) and is likely related

544 to the lack of anthropogenic sources of freshly emitted ozone-precursors and the presence of higher
545 levels of biogenic ozone-precursors, which do not follow anthropogenic cycling. However, the
546 levels of ozone in high mountain environments are also known to be strongly affected by (i) the
547 transport of polluted air masses by local wind systems (valley and slope winds) from the Po Valley
548 and surrounding cities inside the Alps (Kaiser et al., 2009), Foehn wind events (Seibert et al., 2000),
549 large scale synoptic air pollutant transport (Wotawa et al., 2000) and stratospheric inputs
550 (Vingarzan, 2004). Nocturnal dry deposition is also less effective at mountain sites.

551

552 Daily cycles of SO₂ are quite different thorough the region and between site categories and show
553 two different patterns. Most sites present NO_x-like patterns, i.e. two weak peaks corresponding to
554 the morning and evening rush hours. On the contrary, all RUR sites plus all sites in VE (with
555 different categorizations) and VI-URB3 (190 m a.s.l.) exhibited diurnal patterns very similar to
556 ozone, i.e. higher levels in the middle of the day. The two patterns remain different throughout the
557 year: different source emissions and weather factors may explain such patterns. The first cycle is
558 related to road traffic and is more evident at VR-TRA3 (close to a large logistic intermodal freight
559 transport hub), where the highest levels of NO_x are recorded. In Europe, sulphur content in
560 automotive gasoline and diesel is now limited to <10 ppm (since 2009), however it is clear that
561 large volumes in traffic and congestion during rush hours may have a key effect in shaping the
562 diurnal SO₂ levels. The second pattern was previously seen in Venice-Mestre (Masiol et al., 2014c)
563 and was related to local emissions from the nearby industrial zone hosting a large coal-fired power
564 plant and a large oil refinery, which are well known strong sources of SO₂, as indicated by local
565 emission inventories (ISPRA, 2015; ARPAV – Regione Veneto, 2015). The closeness of VE sites
566 to the sea drives the presence of sea/land breezes (mainly in warmest periods) and has a strong
567 influence of the local circulation pattern and in bringing air masses from the industrial zone to the
568 site locations. The daytime increase in SO₂ was also reported for a background site in London by

569 Bigi and Harrison (2010) who attributed it to the downward mixing of plumes from elevated point
570 sources as the boundary layer deepens during daylight hours.

571 Generally, PM₁₀ exhibits higher concentrations overnight and clear minima in the early afternoon.

572 This pattern is consistent with the diurnal dynamics of the mixing layer. However, a secondary
573 cause may be related to the volatilisation of the more volatile aerosol compounds (e.g., nitrate)
574 during the early afternoon, i.e. when the air temperature is higher and relative humidity lower.

575 Minor peaks of PM₁₀ concentrations can be found just before noon at a few sites affecting by very
576 different emission scenarios (VR.URB2, VR.URB3, VE.URB3, PD.RUR2, PD.IND4). Their
577 interpretation is not clear and may be related to the local characteristics of the sites.

578

579 **4.6 Long-term trends**

580 The long-term trends were analysed using the monthly-averaged data: since missing data can
581 significantly affect the trend analysis, only months having at least 75% of available records were
582 processed. In addition, only trends over periods extending more than 4 consecutive years were
583 computed. The quantification and the significance of the trends were evaluated by applying the
584 Theil-Sen nonparametric estimator of slope (Sen, 1968; Theil, 1992). This technique assumes linear
585 trends and is therefore useful to estimate the interannual trends, but it is irrespective of the shape of
586 trends. The slopes were also deseasonalized by using the seasonal trend decomposition using loess
587 (STL) to exclude the effect of the seasonal cycles. Details of STL are provided in Cleveland et al.
588 (1990). The statistics of the linear trends are listed in Table SII as percentage y^{-1} , while Figure SI7
589 shows all the single trends expressed in concentration y^{-1} along with the upper and lower 95th
590 confidence intervals in the trends and the p -values, which indicate the statistical significance of the
591 slope estimation.

592

593 The trends observed at each site reflect both regional and local changes and are affected by the
594 particular characteristics of the site locations. However, when trends observed at individual sites are

595 aggregated at provincial or regional levels, their relationships with current and past emissions
 596 inventories can be examined. The slopes calculated with the Theil-Sen method are then compared
 597 with changes in primary emissions as reported in various emission inventories (EIs) available at
 598 both regional and provincial level.
 599

600 For each pollutant, statistically significant ($p < 0.05$) trends expressed in percentage y^{-1} are provided
 601 in Figure 8 along with: (i) the differences in estimated emissions between 2010 and 2005 at
 602 provincial level provided by the EI SINAnet top-down (ISPRA, 2015) and (ii) the differences
 603 between 2010 and 2007/8 at regional scale provided by INEMAR (ARPAV – Regione Veneto,
 604 2015). Differences of EIs (Δ EIs) are also expressed as percentage y^{-1} for an easier comparison with
 605 measured data (this choice considers a linear trend throughout the considered periods). Generally,
 606 most of the trends are negative for all the species and the changes in measured concentrations of
 607 CO, NO_x, PM₁₀, PM_{2.5} agree well with EIs. However, some exceptions are also found (note that not
 608 all sites revealed statistically significant slopes).
 609

610 CO concentrations decreased significantly at 12 of 18 sites with more than four years of available
 611 data, with slopes between $-20.5\% y^{-1}$ (TV.RUR) and $-1\% y^{-1}$ (PD.IND1). This result is in line with
 612 the average drops by -6.5% reported by INEMAR for the whole Veneto and with the EIs provided
 613 by SINAnet at province scale. However, some sites show the opposite behaviour, i.e. increased
 614 concentrations: BL.URB ($+3.5\% y^{-1}$), VR.URB2 ($+9.6\% y^{-1}$) and VE.TRA2 ($+18.2\% y^{-1}$). Since
 615 falls of CO in EIs are mainly driven by road transport and non-industrial combustion (including
 616 biomass burning), such sites have possibly experienced local increases of road traffic volumes or
 617 emissions from the use of wood for domestic heating, which is widely used in mountain areas
 618 (mainly BL).
 619

620 The average decrease of NO_x levels across the whole region was estimated as $-4.1\% \text{ y}^{-1}$ by
621 INEMAR and was mainly attributed to “road transport” and, secondarily, to “combustion in energy
622 and transformation industry” and “combustion in industry” sectors. The average slope from data
623 measured experimentally at all the sites was $-3.5\% \text{ y}^{-1}$, ranging between $-12.3\% \text{ y}^{-1}$ (VR.IND) and -
624 $1.5\% \text{ y}^{-1}$ (VI.TRA). Statistically significant trends were negative at all sites except at VI.IND
625 ($+1.5\% \text{ y}^{-1}$). This result is a positive finding meaning that abatement strategies and improvement of
626 technologies had an effect in reducing the ambient levels of NO_x . However, in recent years there
627 has been increasing interest in NO_x emissions and NO/NO_2 partitioning in Europe. Evident
628 discrepancies have been found between achieving NO_x emission reductions and NO_2 ambient
629 concentrations, which do not meet the targets in many locations (e.g., Grice et al., 2009; Cyrus et
630 al., 2012). These concerns have been related to the recent increase in NO_2 levels in Europe due to
631 the increased proportion of diesel-powered vehicles, which are known to have higher primary
632 (direct) emissions of NO_2 (Carslaw et al., 2007). Since the recent boom of diesel vehicles was also
633 experienced in Italy (Cames and Helmers, 2013), the relationship between significant trends of NO_x
634 and NO_2 needs to be further investigated.

635

636 Analysis of trends in SO_2 requires particular care. Based on EIs estimations, a significant drop (-
637 $14\% \text{ y}^{-1}$) was experienced across the whole region, while at province level SO_2 emissions decreased
638 between $-18\% \text{ y}^{-1}$ (in RO) and $-6\% \text{ y}^{-1}$ (in BL). These drops in EIs are principally attributed to the
639 sector of combustion in energy transformation industries. In Veneto, this sector is mostly
640 represented by the energy production in coal-fired power stations, which is present in VE province
641 (Porto Marghera). In addition, the sector of ‘other mobile sources’ has also experienced significant
642 drops, particularly of ship emissions (present only in coastal areas of VE province): from January
643 2010, ships in the harbours are requested to use fuels with sulphur content $<0.1\%$. According to the
644 EIs, experimental data show that all sites in the VE province and PD.IND2 have negative trends,
645 while four sites have experienced statistically significant increases in SO_2 levels, i.e. VI.URB3

646 (+24.5% y^{-1}), VR.RUR (+11.4% y^{-1}), PD.TRA (+9.9% y^{-1}) and RO.TRA (+7.4% y^{-1}). While the
647 decline at VE sites may be attributed to the concurrent fall in industrial and maritime source
648 emissions at a local scale, the increases at other sites deserve further investigation and are possibly
649 due to long-range transport of polluted air masses. In this context, a recent study (Masiol et al.,
650 2015) has reported that Eastern Europe is a potential source area for PM_{2.5}-bound sulphate, i.e. the
651 major sink for atmospheric SO₂.

652
653 Measured data fit well with changes in EIs for PM₁₀, except in VI province. All statistically
654 significant trends calculated from field data show decreases in PM₁₀ concentration ranging between
655 -5.6% y^{-1} in BL.RUR2 and -1.9% y^{-1} in RO.TRA. PM₁₀ emissions estimated by EIs dropped
656 between -4.4% y^{-1} in RO province and -2.4% y^{-1} in VR, with a slight increase in VI (+1.1% y^{-1}). At
657 a regional scale, the INEMAR inventory reports an overall decrease of -5.7% y^{-1} . Results for PM_{2.5}
658 are quite variable, mostly due to the short series of available experimental data: only 3 sites present
659 more than 4 years of data, of which only 2 have statistically significant trends. Hence, no further
660 information can be extracted for PM_{2.5}.

661

662 **Conclusions**

663 Air quality data from 43 monitoring sites have been used as input for a number of statistical tools to
664 assess the extent of air pollution across the Veneto. This paper is the first one providing information
665 from a large number of sites over a wide region of N Italy. The main findings can be summarised as
666 follows:

- 667 • Carbon monoxide and sulphur dioxide show low levels across the region and, therefore, are not
668 considered as critical pollutants. While CO does not show any evident spatial trend, SO₂ levels
669 are higher in VE Province, particularly around Venice-Mestre. This anomaly was linked to the
670 industrial zone (coal power plant, oil refineries, other industrial installations) and harbour
671 activities;

- 672 • Nitrogen dioxide, ozone and particulate matter (both PM_{10} and $PM_{2.5}$) are critical pollutants in
673 view of protecting human health, i.e. the EC limit and target values are frequently breached at
674 some sites. Those air pollutants deserve special attention because of their known adverse effects
675 upon public health: future mitigation strategies should focus on reducing concentrations of such
676 key pollutants;
- 677 • Air pollutants are quite uniformly distributed across the region: no pairs of sites have statistically
678 significant differences in the levels of CO, while only the two remote rural sites present
679 statistically significant differences from a large number of other sites for NO_x and ozone;
- 680 • The current site categorization was tested by applying a data depth classification analysis: results
681 show that sites categorized as rural generally differ from other categories, while there is not a
682 clear separation among urban background, traffic and industrial sites. Probable causes of the
683 poor classification are discussed; some insights for improving the monitoring network are
684 provided;
- 685 • Spatial trends were investigated by interpolating average concentrations at the rural sites: despite
686 NO and NO_2 having a slightly different direction of maximum slopes, nitrogen oxides generally
687 increase from the mountain to the coastal plain environments, while ozone presents maxima
688 concentrations at high mountain rural sites and minima in coastal areas;
- 689 • Seasonal pattern analysis revealed that CO, NO, NO_2 , NO_x , PM_{10} and $PM_{2.5}$ show significantly
690 higher levels in colder months and minima in summer. This pattern is mainly attributed to the
691 lower mixing layer heights, the limited oxidation potential and the emissions from domestic
692 heating. The volatilization of semi-volatile aerosol compounds during the warmer seasons is
693 another reason of this behavior for PM. On the contrary, ozone has an opposite seasonality with
694 maxima in summer due to its increased photochemical generation. No seasonal patterns are
695 found for SO_2 ;
- 696 • Diurnal and weekly cycles were investigated. Generally, similar patterns are observed across the
697 region for all the measured species. A strong potential effect of road traffic emissions was found

for CO and nitrogen oxides: one/two daily peaks are commonly found at urban and hotspot sites and were related road traffic emissions during rush hours. Ozone cycles were shaped by the photochemistry and by the interplay with NO. PM cycles generally show higher levels overnight and , therefore, are mostly shaped by the mixing layer height dynamics;

- An overall decrease of all measured species (except ozone) was observed throughout the region. Generally, results of trend analysis well fit with changes in emission inventories. However, some sites with opposite trends have been identified; the reasons for increasing concentrations in such sites needs to be further investigated.

Disclaimer

The views and conclusions expressed in this paper are exclusively of the authors and may not reflect those of ARPAV.

ACKNOWLEDGEMENTS

We gratefully acknowledge: (i) ARPAV for providing data; (ii) the European Environment Agency for providing CORINE Land Cover 2006 data.

REFERENCES

- Agostinelli, C. Romanazzi, M. Local depth. J. Stat. Plan. Inference 2011;141(2):817-830.
- Agostinelli, C. Romanazzi, M. Nonparametric analysis of directional data based on data depth. Environ Ecol Stat 2013; 20(2):253-270.
- ARPAV (Environmental Protection Agency of Veneto Region).). Relazione Regionale Qualità dell'aria – Anno 2011 [in Italian], 2012. Available from: <http://www.arpa.veneto.it/temi-ambientali/aria/riferimenti/documenti/documenti-1> (last accessed: June 2015).
- ARPAV(Environmental Protection Agency of Veneto Region). Relazione Regionale Qualità dell'aria – Anno 2013; 2014 [in Italian]. Available from: <http://www.arpa.veneto.it/temi-ambientali/aria/riferimenti/documenti/documenti-1> (last accessed: June 2015).
- ARPAV (Environmental Protection Agency of Veneto Region) – Regione Veneto. INEMAR VENETO 2010 - Inventario Regionale delle Emissioni in Atmosfera in Regione Veneto, edizione 2010 – Risultati dell'edizione 2010 in versione definitiva – Relazione generale. ARPA Veneto - Osservatorio Regionale Aria, Regione del Veneto - Dipartimento Ambiente, Sezione Tutela Ambiente, Settore Tutela Atmosfera; 2015 [in Italian]. Available at: <http://www.arpa.veneto.it/temi-ambientali/aria/emissioni-di-inquinanti/inventario-emissioni> [last accessed on Nov 2015]
- Anttila P, Tuovinen JP, Niemi JV. Primary NO2 emissions and their role in the development of NO2 concentrations in a traffic environment. Atmos Environ 2011;45(4):986-992.
- Bigi A, Harrison RM. Analysis of the air pollution climate at a central urban background site, Atmos Environ 2010; 44: 2004-2012.

Bigi A, Ghermandi G, Harrison RM. Analysis of the air pollution climate at a background site in the Po valley. *J Environ Monit* 2012;14:552-563.

Cames, M., Helmers, E. Critical evaluation of the European diesel car boom—global comparison, environmental effects and various national strategies. *Environ. Sci. Europe* 2013;25(1):1.

Carslaw DC. The openair manual — open-source tools for analysing air pollution data. Manual for version 28th January 2015, King's College London; 2015.

Carslaw DC, Ropkins K. openair - an R package for air quality data analysis. *Environ Model Softw* 2012;27-28:52-61.

Claeskens G, Hubert M, Slaets L, Vakili K. Multivariate functional halfspace depth. *J Am Stat Assoc* 2014; 109(505):411–423.

Clapp, L.J., Jenkin, M.E. Analysis of the relationship between ambient levels of O₃, NO₂ and NO as a function of NO_x in the UK. *Atmos. Environ.* 2001;35:6391–6405.

Cleveland RB, Cleveland WS, McRae JE, Terpenning I. STL: a seasonal-trend decomposition procedure based on loess. *J Off Stat* 1990;6(1):3–73.

Colette A, Granier C, Hodnebrog Ø, Jakobs H, Maurizi A, Nyiri A, et al. Air quality trends in Europe over the past decade: a first multi-model assessment. *Atmos Chem Phys* 2011;11(22):11657-11678.

Contini D, Gambaro A, Donato A, Cescon P, Cesari D, Merico E, Citron M. Inter-annual trend of the primary contribution of ship emissions to PM_{2.5} concentrations in Venice (Italy): Efficiency of emissions mitigation strategies. *Atmos Environ* 2015;102:183-190.

Cristofanelli P, Bonasoni P, Carboni G, Calzolari F, Casarola L, Sajani SZ, Santaguida R. Anomalous high ozone concentrations recorded at a high mountain station in Italy in summer 2003. *Atmos Environ* 2007;41(7):1383-1394.

Cuevas A. A partial overview of the theory of statistics with functional data. *J. Stat. Plan. Inference* 2014;147:1-23.

Curci G, Beekmann M, Vautard R, Smiatek G, Steinbrecher R, Theloke J, Friedrich R. Modelling study of the impact of isoprene and terpene biogenic emissions on European ozone levels. *Atmos Environ* 2009;43(7):1444-1455.

Cyrus J, Eeftens M, Heinrich J, Ampe C, Armengaud A, Beelen R, et al. Variation of NO₂ and NO_x concentrations between and within 36 European study areas: results from the ESCAPE study. *Atmos Environ* 2012;62:374-390.

Demšar J. Statistical comparisons of classifiers over multiple data sets. *J Mach Learn Res* 2006;7:1-30.

Di Giuseppe F, Riccio A, Caporaso L, Bonafe G, Gobbi GP, Angelini F. Automatic detection of atmospheric boundary layer height using ceilometers backscatter data assisted by a boundary layer model. *Q J R Meteorol Soc* 2012;138:649-663.

Duane M, Poma B, Rembges D, Astorga C, Larsen BR. Isoprene and its degradation products as strong ozone precursors in Insubria, Northern Italy. *Atmos Environ* 2002;36(24):3867-3879.

EEA (European Environment Agency). AirBased The European Air Quality Database. <http://www.eea.europa.eu/themes/air/air-quality/map/airbase>, 2016 (accessed February 2016).

Gentner DR, Worton DR, Isaacman G, Davis LC, Dallmann TR, Wood EC, et al. Chemical composition of gas-phase organic carbon emissions from motor vehicles and implications for ozone production. *Environ Sci Technol* 2013;47(20):11837-11848.

Grice, S., Stedman, J., Kent, A., Hobson, M., Norris, J., Abbott, J., Cooke, S.. Recent trends and projections of primary NO₂ emissions in Europe. *Atmos. Environ.* 2009;43:2154-2167.

JRC- AQUILA. Position Paper - Assessment on siting criteria, classification and representativeness of air quality monitoring stations. Available at: <http://ec.europa.eu/environment/air/pdf/SCREAM%20final.pdf> [last accessed: April 2016]

Kaiser A. Origin of polluted air masses in the Alps. An overview and first results for MONARPOP. *Environ Pollut* 2009;157(12):3232-3237.

Keuken MP, Roemer MGM, Zandveld P, Verbeek RP, Velders GJM. Trends in primary NO₂ and exhaust PM emissions from road traffic for the period 2000–2020 and implications for air quality and health in the Netherlands. *Atmos Environ* 2012;54:313-319.

Khan MB, Masiol M, Formenton G, Di Gilio A, de Gennaro G, Agostinelli C, Pavoni B. Carbonaceous PM_{2.5} and secondary organic aerosol across the Veneto region (NE Italy). *Sci Total Environ* 2016;542:172-181.

Kley D, Kleinmann M, Sanderman H, Krupa S. Photochemical oxidants: state of the science. *Environ Pollut* 1999;100:19-42.

Kurtenbach R, Kleffmann J, Niedojadlo A, Wiesen P. Primary NO₂ emissions and their impact on air quality in traffic environments in Germany. *Environ Sci Europe* 2012;24(12):1-8.

ISPRA, Italian Institute for Environmental Protection and Research. Disaggregated emission inventory. <http://www.sinanet.isprambiente.it/it/inventaria/disaggregazione-dellinventario-nazionale-2010>, 2015 (accessed 30 October 2015).

Lenschow, P., Abraham, H.-J., Kutzner, K., Lutz, M., Preuß, J.-D., Reichenbacher, W. Some ideas about the sources of PM₁₀. *Atmos Environ* 2001;35:S23–S33.

Li J, Cuesta-Albertos JA, Liu RY. DD-classifier: Nonparametric classification procedures based on DD-plot. *J Am Stat Assoc* 2012;107:737–753.

Liu RY. On a Notion of Data Depth Based on Random Simplices. *The Annals of Statistics* 1990;18(1):405-414.

797 Lopez-Pintado S, and Romo J. On the Concept of Depth for Functional Data. *Journal of the American Statistical*
798 *Association* 2009;104(486):718–734.

799 Lopez-Pintado S, and Romo, J. A half-region depth for functional data. *Computational Statistics and Data Analysis*
800 2011;55(4):1679–1695.

801 Masiol, M., Centanni, E., Squizzato, S., Hofer, A., Pecorari, E., Rampazzo, G., Pavoni, B. GC-MS analyses and
802 chemometric processing to discriminate the local and long-distance sources of PAHs associated to
803 atmospheric PM_{2.5}. *Environ. Sci. Pollut. Res.* 2012;19(8):3142-3151.

804 Masiol M, Formenton G, Pasqualetto A, Pavoni B. Seasonal trends and spatial variations of PM₁₀-bounded polycyclic
805 aromatic hydrocarbons in Veneto Region, Northeast Italy. *Atmos Environ* 2013;79:811-821.

806 Masiol M, Formenton G, Giraldo G, Pasqualetto A, Tieppo P, Pavoni B. The dark side of the tradition: the polluting
807 effect of Epiphany folk fires in the eastern Po Valley (Italy). *Sci Total Environ* 2014a;473-474: 549-564.

808 Masiol, M., Squizzato, S., Rampazzo, G., Pavoni, B. Source apportionment of PM_{2.5} at multiple sites in Venice (Italy):
809 Spatial variability and the role of weather. *Atmos. Environ.* 2014b;98:78-88.

810 Masiol M, Agostinelli C, Formenton G, Tarabotti E, Pavoni B. Thirteen years of air pollution hourly monitoring in a
811 large city: Potential sources, trends, cycles and effects of car-free days. *Sci Total Environ* 2014c;494–
812 495:84–96.

813 Masiol M, Benetello F, Harrison RM, Formenton G, De Gasperi F, Pavoni B. Spatial, seasonal trends and
814 transboundary transport of PM_{2.5} inorganic ions in the Veneto Region (Northeastern Italy). *Atmos Environ*
815 2015;117:19–31.

816 Mosler K, Polyakova Y. General notions of depth for functional data. *arXiv* 2012; arXiv:1208.1981.

817 Munir S, Chen H, Ropkins K. Modelling the impact of road traffic on ground level ozone concentration using a quantile
818 regression approach. *Atmos Environ* 2012;60:283-291.

819 Pohlert, T. PMCMR: Calculate Pairwise Multiple Comparisons of Mean Rank Sums. R package version 1.3.
820 <http://CRAN.R-project.org/package=PMCMR>, 2015.

821

822 Putaud JP, Raes F, van Dingenen R, Brüggemann E, Facchini M C, Decesari S, et al. A European aerosol
823 phenomenology – 2: chemical characteristics of particulate matter at kerbside, urban, rural and background
824 sites in Europe. *Atmos Environ* 2004;38:2579–2595.

825 Putaud, JP, Van Dingenen R, Alastuey A, Bauer H, Birmili W, Cyrys J, et al. A European aerosol phenomenology – 3:
826 Physical and chemical characteristics of particulate matter from 60 rural, urban, and kerbside sites across
827 Europe. *Atmos Environ* 2010;44:1308–1320.

828 R Core Team. R: A language and environment for statistical computing. R Foundation for Statistical Computing,
829 Vienna, Austria, 2016. URL <https://www.R-project.org/>.

830 Ramsay JO, Silverman BW. *Functional Data Analysis*. Springer, 2006.

831 Romano, B., Zullo, F. Half a century of urbanization in southern European lowlands: a study on the Po Valley
832 (Northern Italy). *Urban Res. Practice* 2015; 8:1-22.

833 Seibert P, Feldmann H, Neiningen B, Bäumle M, Trickl T. South foehn and ozone in the Eastern Alps–case study and
834 climatological aspects. *Atmos Environ* 2009;34(9):1379-1394.

835 Sen PK. Estimates of the regression coefficient based on Kendall's tau. *J Am Stat Assoc* 1968;63:1379-1389.

836 Squizzato, S., Masiol, M., Visin, F., Canal, A., Rampazzo, G., Pavoni, B. The PM_{2.5} chemical composition in an
837 industrial zone included in a large urban settlement: main sources and local background. *Environ. Sci.*
838 *Process. Impacts* 2014;16:1913-1922.

839 Theil H. A rank-invariant method of linear and polynomial regression analysis. In: *Henri Theil's Contributions to*
840 *Economics and Econometrics*. Springer, Netherlands, pp. 345-381; 1992.

841 Vecchi R, Valli G. Ozone assessment in the southern part of the Alps. *Atmos Environ* 1998; 33(1):97-109.

842 Vecchi R, Valli G, Fermo P, D'Alessandro A, Piazzalunga A, Bernardoni V. Organic and inorganic sampling artefacts
843 assessment. *Atmos Environ* 2009;43:1713-1720.

844 Vingarzan R. A review of surface ozone background levels and trends. *Atmos Environ* 2004; 38: 3431-3442.

845 Wotawa G, Kröger H, Stohl A. Transport of ozone towards the Alps–results from trajectory analyses and photochemical
846 model studies. *Atmos Environ* 2000;34(9):1367-1377.

847 WHO (World Health Organization). *Air Quality Guidelines for Europe*. European Series No 91, World Health
848 Organization. WHO Regional Publications, Geneva; 2000.

849 Zhu, T., Melamed, M., Parrish, D., Gauss, M., Klenner, L.G., Lawrence, M., Konare, A. Lioussé, C., 2012. Impacts of
850 Megacities on Air Pollution and Climate. WMO, Geneva.

851 Zuo Y, Serfling, RJ. General notions of statistical depth function. *The Annals of Statistics* 2000;28(2):461-482.

852 **Table 1.** Characteristics of the sampling sites and analysed pollutants. Municipality refers to the territorial district where the sampling site is located: if
853 the site is not located in the main town of a municipality, the city/town is given in brackets.
854

Province	No.	Code	Lat.	Long.	Height (m)	Municipality (City/Town)	Site full name	Area type	Monitored pollutants
BL	1	BL.RUR1	46.339	11.802	2020	Falcade	Passo Valles	Rural background	NOx, O3
	2	BL.RUR2	46.163	12.361	615	Pieve d'Alpago	Pieve d'Alpago	Rural background	NOx, O3, SO2, PM10,
	3	BL.SUB	46.031	11.906	263	Feltre	Area Feltrina	Suburban	CO, NOx, O3, SO2, PM10
	4	BL.URB	46.144	12.219	401	Belluno	BL-città	Urban background	CO, NOx, O3, SO2, PM10
TV	5	TV.RUR	45.837	12.51	14	Treviso (Mansuè)	Mansuè	Rural background	CO, NOx, O3 PM10
	6	TV.URB1	45.672	12.238	15	Treviso	TV-Via Lancieri	Urban background	CO, NOx, O3, SO2, PM10, PM2.5
	7	TV.URB2	45.89	12.307	72	Conegliano	Conegliano	Urban background	CO, NOx, O3, SO2, PM10
VI	8	VI.RUR	45.849	11.569	1366	Asiago	Asiago-Cima Ekar	Rural background	NOx, O3
	9	VI.URB4	45.759	11.736	114	Bassano	Bassano del Grappa	Urban background	NOx, O3 PM10
	10	VI.URB1	45.56	11.539	36	Vicenza	VI-Quartiere Italia	Urban background	CO, NOx, O3
	11	VI.URB2	45.532	11.522	33	Vicenza	VI-Ferrovieri	Urban background	CO, NOx, O3, SO2
	12	VI.URB3	45.714	11.368	190	Schio	Schio-via Vecellio	Urban background	NOx, O3 PM10, PM2.5
	13	VI.TRA	45.545	11.533	35	Vicenza	VI-San Felice	Urban-traffic	CO, NOx SO2, PM10
	14	VI.IND1	45.536	11.294	154	Chiampo	Chiampo	Urban-industrial	NOx
	15	VI.IND2	45.465	11.386	61	Montebello Vicentino	Montebello Vicentino	Suburban-Industrial	NOx
VR	16	VR.RUR	45.589	11.037	824	Boscochiesanuova	Boscochiesanuova	Rural background	CO, NOx, O3, SO2, PM10
	17	VR.SUB	45.462	10.911	91	Verona (Cason del Chievo)	VR-Cason	Suburban	CO, NOx, O3, SO2, PM10, PM2.5
	18	VR.URB1	45.443	11.007	64	Verona	VR-Piazza Bernardi	Urban background	CO, NOx
	19	VR.URB2	45.399	11.285	30	Verona (San Bonifacio)	San Bonifacio	Urban background	CO, NOx, O3, SO2, PM10, PM2.5
	20	VR.URB3	45.183	11.311	25	Legnago	Legnago	Urban background	NOx, O3 PM10
	21	VR.TRA1	45.444	10.963	62	Verona	VR-Borgo Milano	Urban-traffic	CO, NOx SO2, PM10
	22	VR.TRA2	45.41	10.989	60	Verona	VR-San Giacomo	Urban-traffic	CO, NOx SO2
	23	VR.TRA3	45.416	10.969	65	Verona	VR-ZAI	Urban-traffic	CO, NOx, O3, SO2
	24	VR.IND	45.543	10.886	183	Fumane	Fumane	Industrial	NOx SO2, PM10,
VE	25	VE.RUR	45.694	12.786	5	Concordia Sagittaria	Concordia Sagittaria	Rural background	NOx, O3
	26	VE.URB1	45.428	12.313	1	Venezia	VE-Sacca Fisola	Urban background	NOx, O3, SO2, PM10
	27	VE.URB2	45.5	12.261	1	Venezia (Mestre)	VE-Parco Bissuola	Urban background	CO, NOx, O3, SO2, PM10
	28	VE.URB3	45.629	12.59	3	San Donà di Piave	San Donà di Piave	Urban background	CO, NOx, O3 PM10, PM2.5

	29	VE.TRA1	45.49	12.218	2	Venezia (Mestre)	VE-Via Tagliamento	Urban-traffic	CO, NOx SO2, PM10
	30	VE.TRA2	45.474	12.22	2	Venezia (Marghera)	VE-Via Beccaria	Urban-traffic	CO, NOx , PM10
	31	VE.IND	45.438	12.205	2	Venezia (Marghera)	VE-Malcontenta	Industrial	CO, NOx SO2
PD	32	PD.RUR1	45.594	11.909	24	Santa Giustina in Colle	S. Giustina in Colle	Rural background	CO, NOx, O3
	33	PD.RUR2	45.289	11.642	18	Padova (Cinto Euganeo)	Parco Colli Euganei	Rural background	NOx, O3, SO2, PM10
	34	PD.URB	45.371	11.841	13	Padova	PD-Mandria	Urban background	CO, NOx, O3, SO2, PM10
	35	PD.TRA	45.433	11.89	11	Padova	PD-Arcella	Urban-traffic	CO, NOx, O3, SO2, PM10
	36	PD.IND1	45.395	11.909	10	Padova	PD-APS-1-Ignoto	Urban-industrial	CO, NOx, O3, SO2, PM10, PM2.5
	37	PD.IND2	45.415	11.907	10	Padova	PD-APS-2-Carli	Urban-industrial	CO, NOx, O3, SO2, PM10, PM2.5
	38	PD.IND3	45.378	11.94	8	Padova	PD-Granze	Urban-industrial	PM10
	39	PD.IND4	45.227	11.666	12	Este	Este	Suburban-Industrial	CO, NOx, O3, SO2, PM10
RO	40	RO.RUR	45.103	11.554	8	Badia Polesine	Polesine-Villafora	Rural background	CO, NOx, O3, SO2
	41	RO.SUB	44.95	12.333	1	Porto Tolle	Porto Tolle	Suburban	NOx SO2, PM10, PM2.5
	42	RO.URB	45.039	11.79	3	Rovigo	RO-Borsea	Urban background	CO, NOx, O3, SO2
	43	RO.TRA	45.074	11.782	7	Rovigo	RO-Centro	Urban-traffic	CO, NOx, O3, SO2, PM10

855

856

857

858

859

860

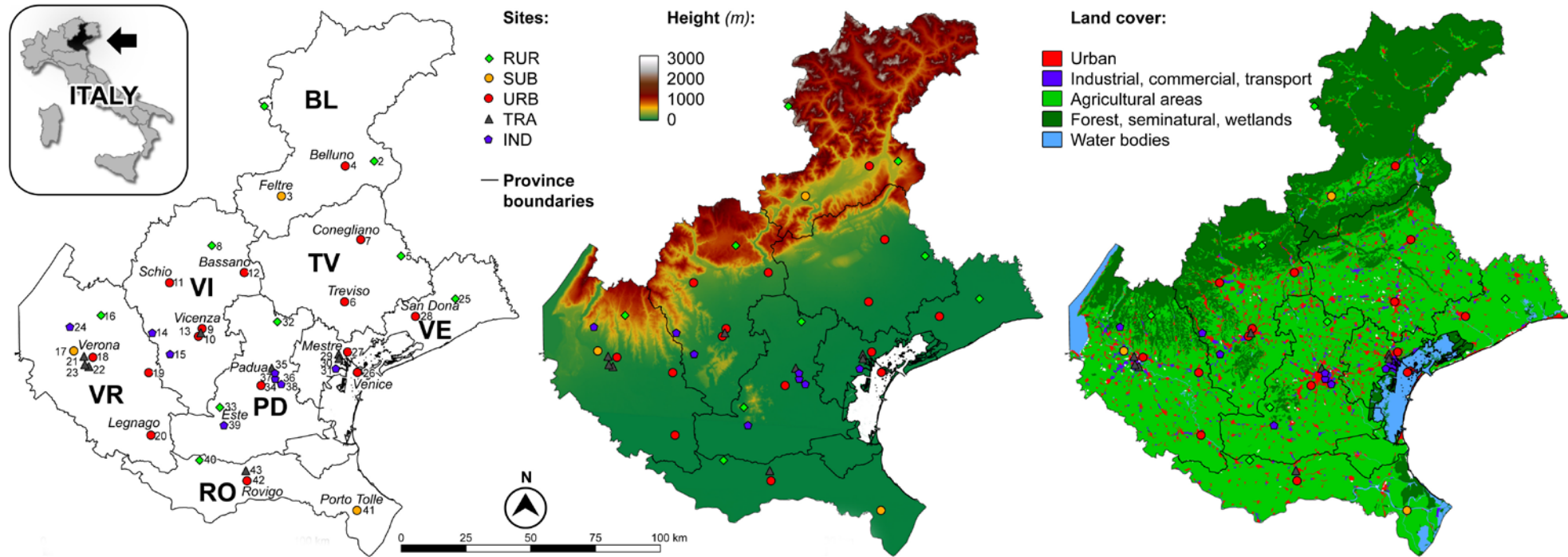
861

862

863

864

865



867

868

869

870

Figure 1. Map of the Veneto Region: administrative (left); terrain relief (centre); land use and cover from CORINE Land Cover 2006 data (right). Sampling sites are also represented as diamonds (RUR sites), dots (SUB and URB sites), triangles (TRA sites) and pentagons (IND sites).

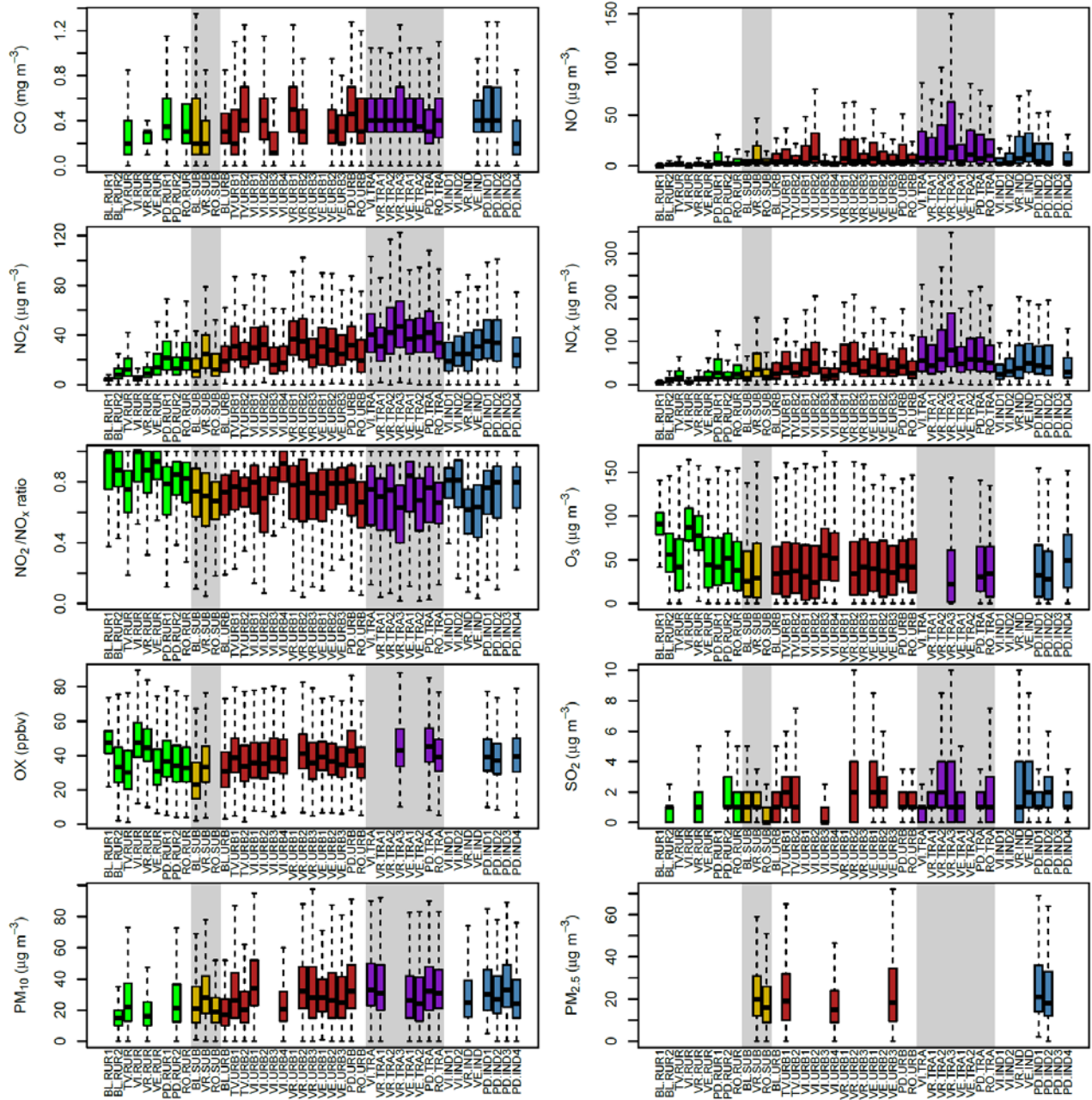


Figure 2. Average and ranges of concentrations of the analyzed pollutants as boxplots of raw data (line= median, box= inter-quartile range, whiskers= $\pm 1.5 \times$ inter-quartile range). Sites are clustered following their categorisation.

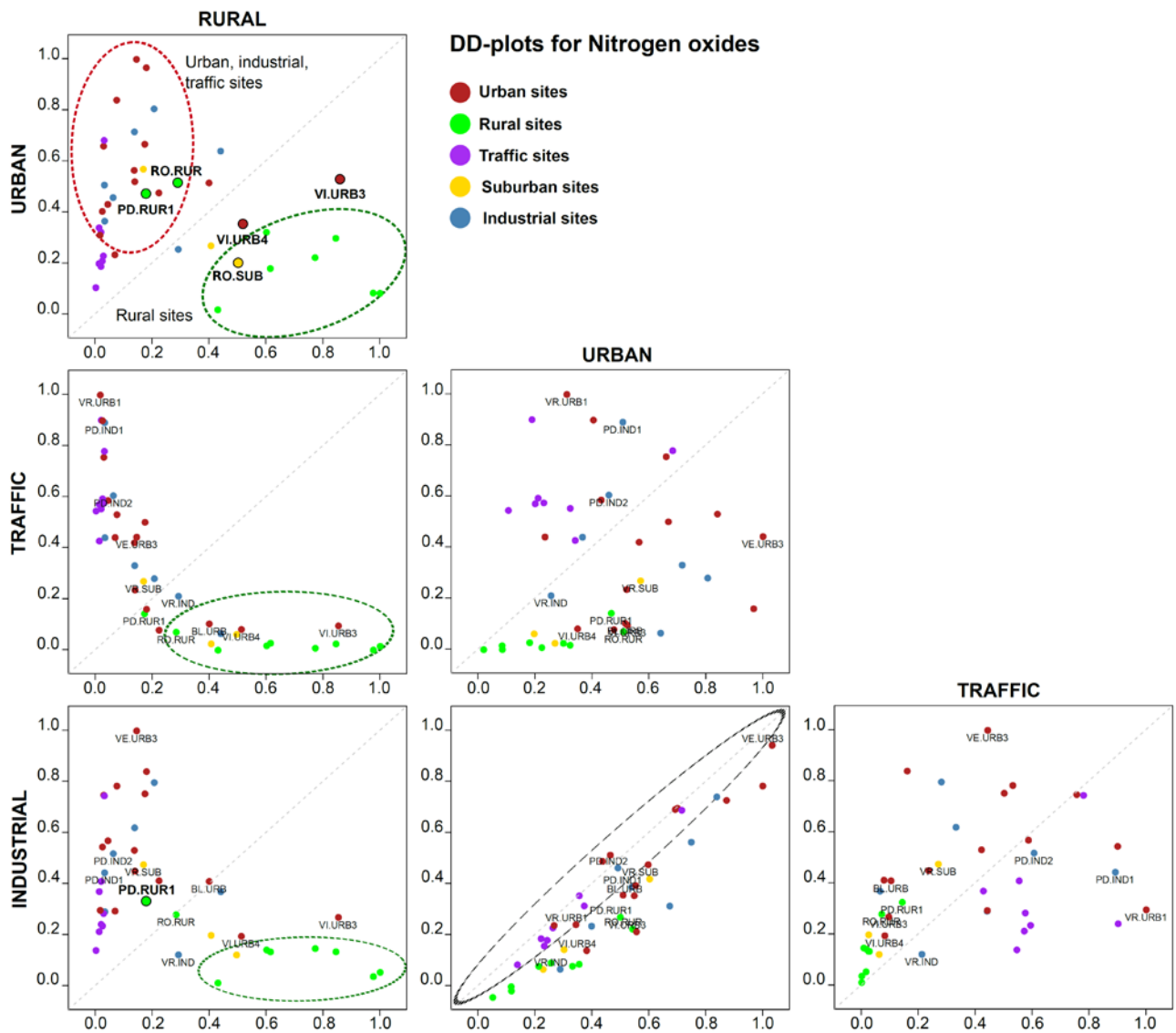


Figure 3. Classification of the stations based DD-plot for nitrogen oxides. The analysis is based on multivariate functional simplicial data depth using nitrogen oxides (NO , NO_2 and NO_x).

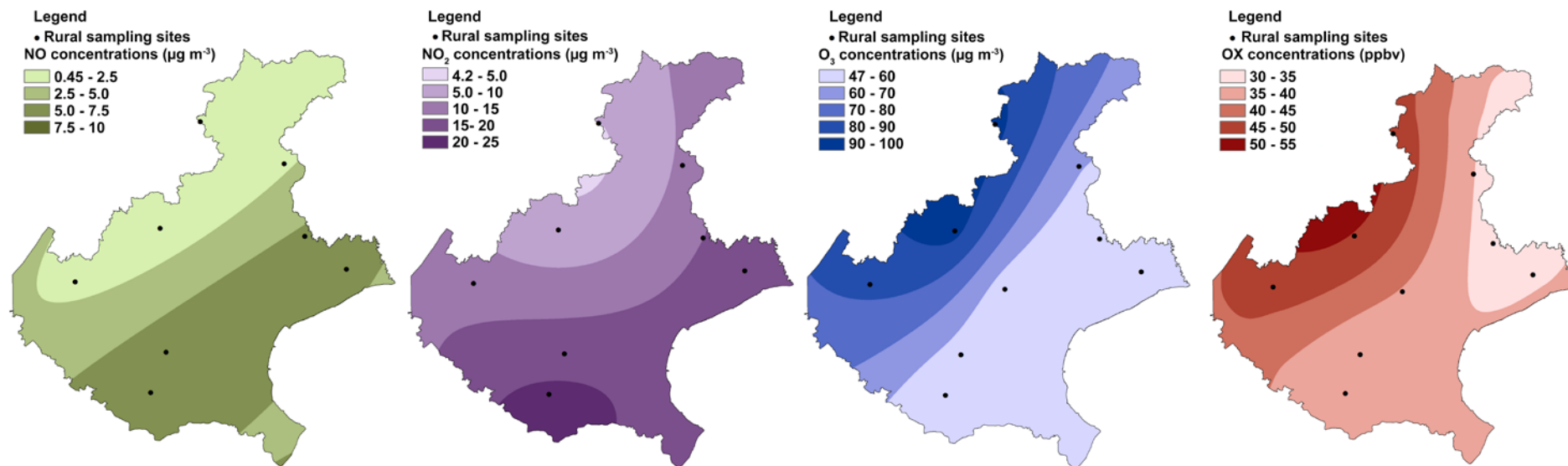


Figure 4. Maps of concentrations for NO, NO₂, O₃ and OX measured at the RUR sites. All RUR sites were used to interpolate data for O₃ and OX, while PD-RUR1 was not used for NO and NO₂ because of the anomalously high levels recorded. Ordinary kriging method was used for interpolation. Maps showing the standard errors associated with predictions are shown as Figure SI5.

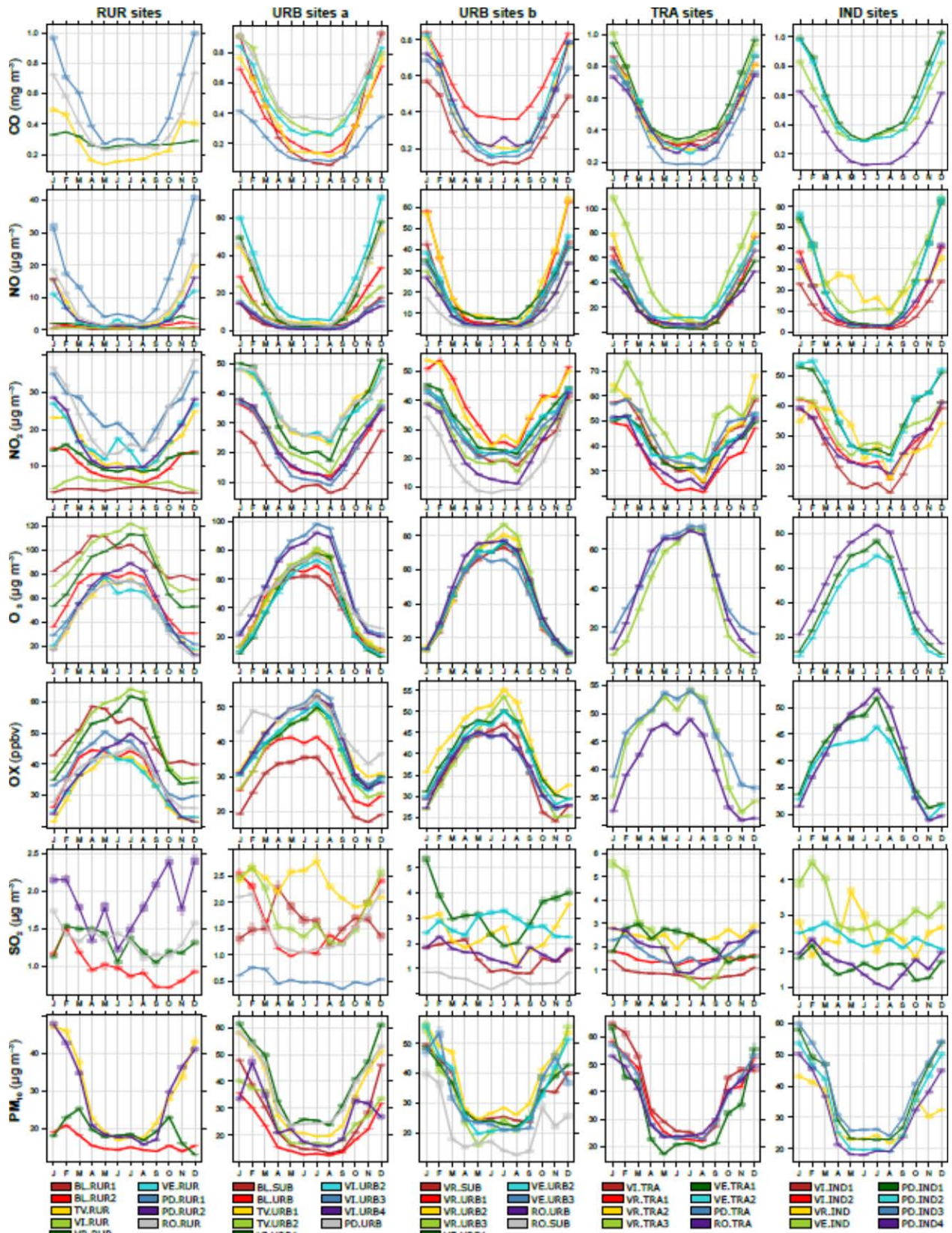


Figure 5. Seasonal variations of the monitored pollutants. Each plot reports the monthly average levels as a filled line and the associated 75th and 99th confidence intervals calculated by bootstrapping the data (n=200).

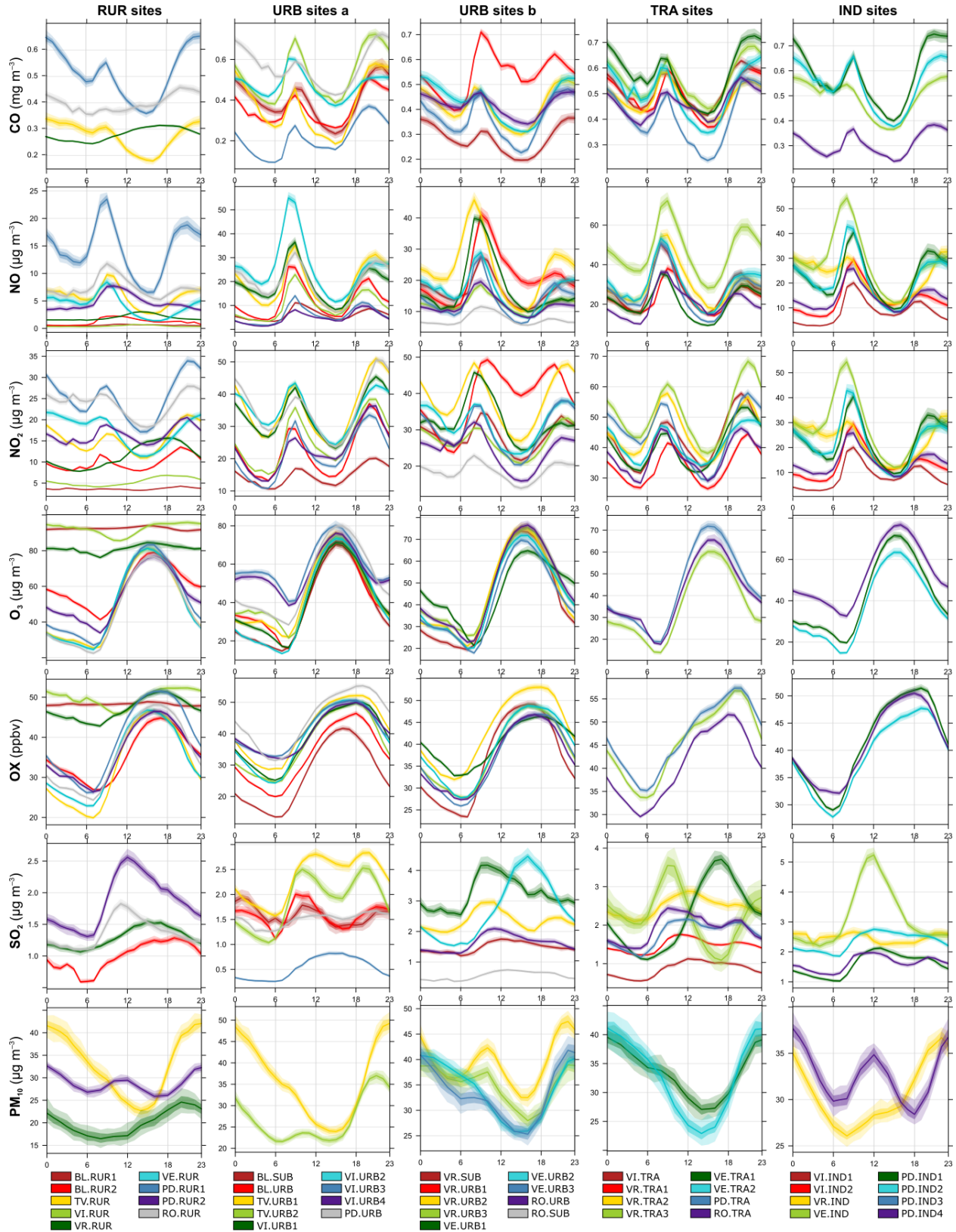


Figure 6. Diurnal variations of levels of measured pollutants computed over the hourly averaged data during the sampling period. Each plot reports the average level as a filled line and the associated 75th and 99th confidence intervals calculated by bootstrapping the data ($n=200$). Data are corrected for DST.

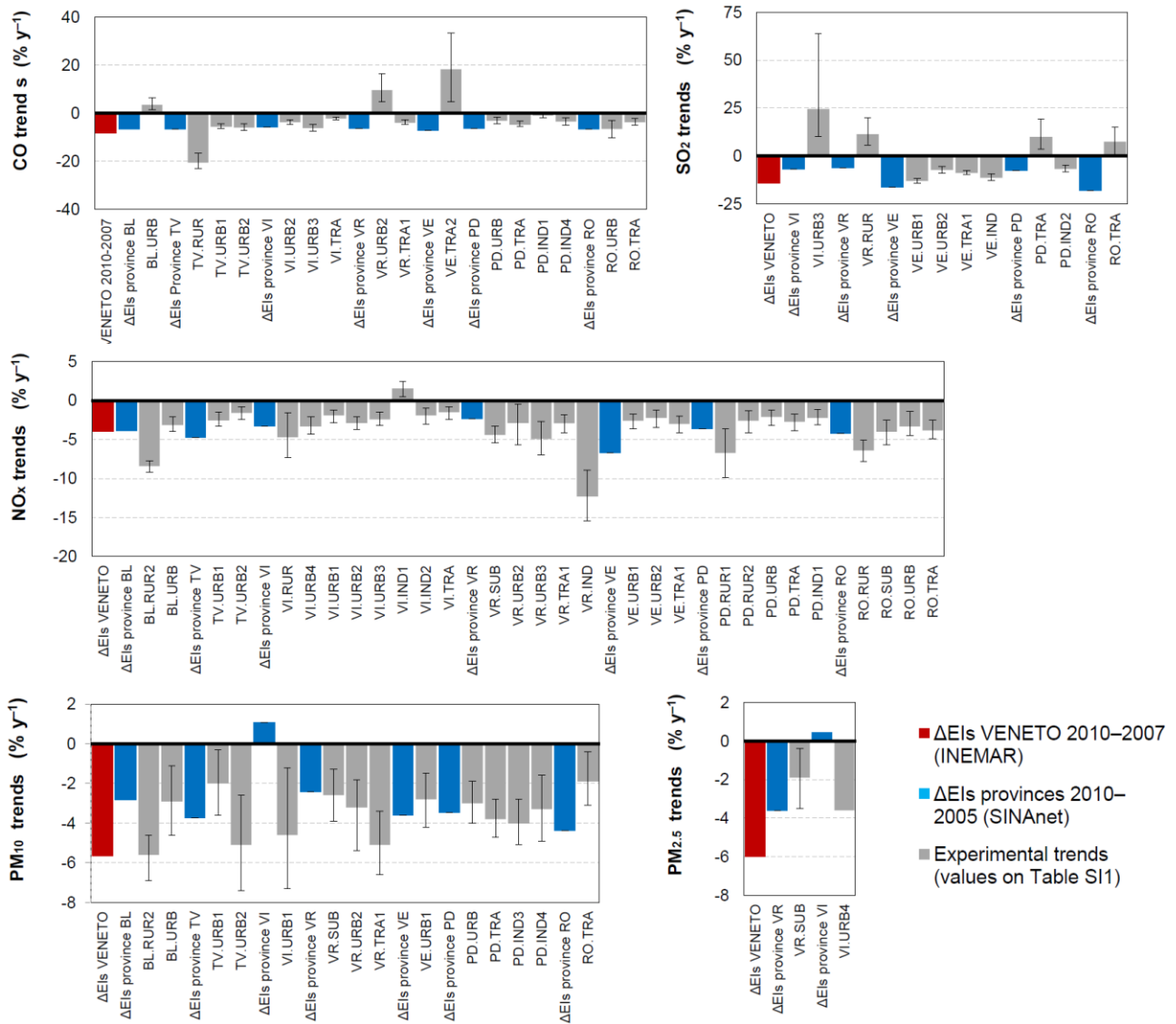


Figure 7. Results of the Theil-Sen analysis of trends (grey bars). The estimated trends are expressed as percentage; the confidence intervals of trends are given by error bars. Only sites showing significant trends (p -values < 0.05) are shown. The percentages of change in emissions provided by the most recent emission inventories are also provided and expressed as $\% \text{ y}^{-1}$: changes of EIs for the whole Veneto region (Δ_{Veneto} , red bars) refers to the difference of EIs between 2010 and 2007; changes of EIs for each province (Δ_{BL} , Δ_{TV} , Δ_{VI} , Δ_{VR} , Δ_{VE} , Δ_{PD} , Δ_{RO} , blue bars) refers to the difference of EIs between 2010 and 2005.